Electroless Deposition of Silver by Galvanic Displacement on Aluminum Alloyed with Copper

Dmitri A. Brevnov,* Tim S. Olson, Gabriel P. López, and Plamen Atanassov

Department of Chemical and Nuclear Engineering, Center for Micro-Engineered Materials, The University of New Mexico, Albuquerque, New Mexico 87131

Received: July 1, 2004; In Final Form: August 23, 2004

In this paper, a procedure is described for the electroless deposition of silver on films containing 99.5% aluminum and 0.5% copper. The deposition proceeds in the absence of external reducing agents via the galvanic displacement mechanism by which silver cations are reduced and copper is oxidized. Although aluminum is a stronger reducing agent than copper, the galvanic displacement of aluminum by silver is not observed with pure (99.997%) aluminum substrates. By alloying aluminum with copper, aluminum films are made amenable to electroless deposition of silver by galvanic displacement. To generate a clean surface for electroless deposition with a controlled and minimal thickness of surface oxide, the aluminum films alloyed with copper are anodized in oxalic acid and etched in a mixture of chromic and phosphoric acids. Thinning of the barrier aluminum oxide during etching and deposition of silver particles are monitored with electrochemical impedance spectroscopy (EIS). Analysis of EIS data indicates that deposition of silver particles for 3 h dramatically increases the interfacial capacitance from 5 to 6 μF/cm^2, characteristic for a thin layer of barrier aluminum oxide, to 30−40 μF/cm^2, typical for metal electrode surfaces. Scanning electron micrographs show that electroless deposition results in the formation of films composed of silver particles. These films can be employed for the fabrication of miniature silver−zinc batteries, optical devices for surface enhanced Raman scattering and FT-IR spectroscopy, composite materials with photocatalytic properties, and surfaces with anti-microbial properties.

Introduction

The electroless deposition of metals (e.g., Au, Ag, and Cu) by galvanic displacement on semiconductor or metal surfaces is a well-known process.[1] This deposition process proceeds via two concurrent electrochemical reactions, which involve the reduction of metal ions and the oxidation of the substrate surface. The driving force for this process is determined by a difference in half-cell potentials (e.g., redox potentials for corresponding metal/metal ion and oxidized substrate/substrate pairs). The half-cell potential of the reduced species must be more positive than that of the oxidized substrate. Chemical etching, which effectively removes the surface layer of oxide, precedes and/or coincides with the deposition of a metal film. Galvanic displacement has been reported for deposition of Au on Si,[2,3] Au on Ge,[4] Pt on Ge,[4] Cu on TaN,[5−7] Cu on Si,[8] Cu on Al,[9] Zn on Al,[10,11] Ni on Al,[12] and other combinations.[2]

In this paper, we report the electroless deposition of silver by the galvanic displacement mechanism on 99.5% aluminum films containing 0.5% copper. Thinning of the layer of aluminum oxide and electroless deposition of silver are carried out in an acidic electrolyte (a mixture of chromic and phosphoric acids). The electroless deposition of zinc by galvanic displacement on aluminum has been previously described and performed by using chemical etching in an alkaline solution of NaOH.[10,11] The zincate activation is typically used as the first step for electroless deposition of other metals (e.g., Ni) on aluminum.[11] Although the zincate activation of the aluminum surface is a well-established and widely used process, little is known about the displacement electroless deposition of silver on aluminum and aluminum alloyed with copper films in acidic media.

Films of silver on aluminum can be utilized in a number of diverse applications, including, for example, miniature silver−zinc batteries.[13] The electroless deposition of silver can also be used to fabricate optical devices for surface enhanced FT-IR spectroscopy,[14] surface enhanced Raman scattering,[15,16] and metal-enhanced fluorescence.[17] In addition, composite materials with silver particles are shown to have useful photocatalytic,[18] anti-microbial properties,[19] and tunable surface plasmon resonances.[20] It is worthwhile to note that the galvanic displacement mechanism is used for a number of technologically important applications. For example, the electroless deposition of Cu on TaN barrier layers is utilized for fabrication of interconnects in ultralarge scale integrated (ULSI) circuits.[5−7] In this case, the electroless deposition of Cu is preceded by the wet etching of the surface oxide with fluoride-containing solutions. The electroless deposition of Cu by the galvanic displacement mechanism is of technological interest for two reasons. This process allows for fabrication of, first, conformal and, second, substrate sensitive deposits.[5−7] In addition to its application for design of interconnects, the electroless deposition by galvanic displacement is important for metallization of silicon based micro-electro-mechanical systems (MEMS).[8]

The objectives of this study are to establish a protocol for the electroless deposition of silver by galvanic displacement on 99.5% aluminum−0.5% copper films and develop a method for in situ monitoring of this process. We show that the electroless deposition can be conveniently monitored by electrochemical impedance spectroscopy (EIS). In addition, we attempt to

* Corresponding author. E-mail: dbrevnov@unm.edu.

10.1021/jp047096u CCC: $27.50
Published on Web 10/19/2004

elucidate the mechanism of silver electroless deposition. The electroless deposition is investigated by interrupting the process and examining the number and size of deposited silver particles as a function of time.

Experimental Section

The samples with particle-type films of silver on aluminum alloyed with copper were fabricated according to the following procedure. First, a 600 nm thick layer of SiO_2 was thermally grown by steam oxidation of a Si wafer. Second, a 3 micron thick layer (99.5 wt % aluminum and 0.5 wt % copper) was deposited on the layer of SiO_2 by physical vapor deposition (PVD). The first and second steps were performed at Sandia National Laboratories (Albuquerque, NM). Third, the sample was anodized in an electrochemical cell, described in detail elsewhere,[21] at 50 V DC for 20 min in 3% w/v oxalic acid at 0 °C. Fourth, the porous and barrier aluminum oxides were etched in a mixture of 0.4 M phosphoric and 0.2 M chromic acids at 60 °C for approximately 2 h. Fifth, $AgNO_3$ was added to the etching solution to obtain a 1.1 mM concentration of Ag+. Electroless deposition of silver was carried out at 60 °C and with no stirring.

Anodization of aluminum films was carried out with a platinum mesh counter electrode and a Hewlett-Packard 4140B pA meter/DC voltage source. EIS experiments were performed in a three-electrode cell with the same working and counter electrodes and a platinum wire as a quasi-reference electrode. EIS was carried out with an IM6-e impedance measurement unit (BAS-Zahner) and the acquired EIS data were analyzed with impedance modeling software (BAS-Zahner). EIS data were acquired at open circuit potential (OCP) over a frequency range between 1 Hz and 100 kHz and with an AC potential amplitude of 5 mV. A low amplitude of AC potential is customarily employed in EIS in order to satisfy the condition of linearity. The impedance data were normalized to the geometric electrode area, 1.4 cm^2. The surface morphology of deposited silver films was evaluated by a Hitachi (S-5200) scanning electron microscope equipped with a PGT spectrometer for energy dispersive spectroscopy (EDS). The microscope was operated at 5−6 kV for imaging and at 25 kV for EDS.

Results and Discussion

The anodization of 99.5% aluminum films containing 0.5% copper and subsequent etching generated a clean surface with a layer of barrier aluminum oxide of defined thickness. Although anodization forms both barrier and porous aluminum oxide layers, etching results in complete dissolution of porous aluminum oxide and partial dissolution of barrier aluminum oxide. Figure 1 demonstrates the Bode representation of an EIS spectrum collected after anodization for 20 min and etching for 110 minutes. An equivalent circuit used for modeling is shown as the insert in Figure 1. The total cell impedance can be modeled as two parallel combinations of a constant phase element (CPE) and a resistor (R) connected in series with each other and the cell uncompensated resistance.[21] The CPE is frequently used instead of a pure capacitance to describe interfacial dielectric properties. One of two parallel (R_1 CPE_1) combinations is readily attributed to the layer of barrier aluminum oxide. In this case, CPE_1 describes the dielectric properties of barrier aluminum oxide and R_1 describes the resistance to ion migration through the barrier aluminum oxide. In previous publications,[22−24] the equivalent circuit used for modeling of EIS data acquired at OCP includes only a single (R CPE) combination. This circuit adequately models the EIS

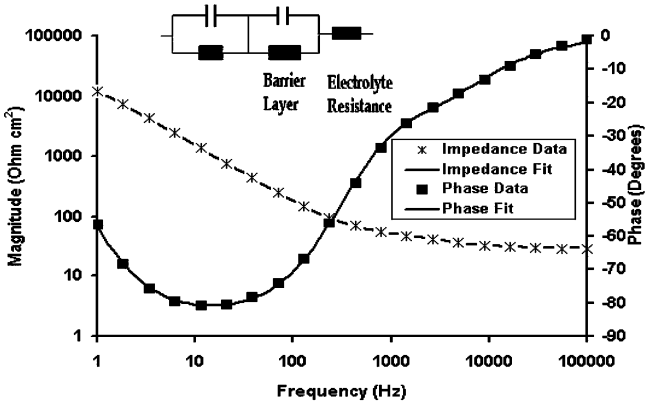

Figure 1. EIS data (magnitude of impedance and phase) collected at OCP after anodization at 50 V, for 20 min in 3% w/v oxalic acid, at 0 °C and subsequent etching a mixture of 0.4 M phosphoric and 0.2 M chromic acids at 60 °C for 110 minutes. The equivalent circuit is shown as an insert.

TABLE 1: Results of Modeling of EIS Data

elements	anodization and etching (Figure 1)	silver deposition (Figure 3)
R_u/Ω	27.6 ± 0.6	14.6 ± 0.6
$R_1/k\Omega\ cm^2$	102 ± 4	1.36 ± 0.14
$CPE_1/\mu F \times s^{\alpha-1}/cm^2$	5.74 ± 0.06	41.6 ± 1.7
α_1	0.968 ± 0.001	0.968 ± 0.005
$R_2/\Omega\ cm^2$	15.1 ± 0.8	13.8 ± 0.8
$CPE_2/\mu F \times s^{\alpha-1}/cm^2$	10.2 ± 0.6	5.2 ± 0.5
α_2	0.712 ± 0.008	0.777 ± 0.008

data only for thick layers of barrier aluminum oxide. If the thickness of this layer is less than approximately 5 nm, significantly better convergence of the overall EIS data fit can be obtained with the introduction of the second (R_2 CPE_2) combination. Although the exact physical origin of the second (R_2 CPE_2) combination is uncertain,[21,25] its introduction to the equivalent circuit is necessary in order to obtain a more accurate estimate of CPE_1 associated with barrier aluminum oxide as shown in Table 1 (left column). The presence of two (R CPE) combinations may be attributed to a two-layer structure of the aluminum oxide film.[26] In this case, the first (R_1 CPE_1) combination represents the outer layer of barrier aluminum oxide with the dielectric constant of 8.6.[21] The second (R_2 CPE_2) combination possibly represents the inner layer of aluminum oxide with different dielectric properties, which is located between the aluminum phase and outer layer of barrier aluminum oxide.[21]

The etching of the layer of barrier aluminum oxide was followed by EIS measurements. The thickness of the barrier oxide layer was calculated according to eq 1, where C_{bl} is capacitance of the barrier aluminum oxide, d is its thickness, A is the geometric surface area, 1.4 cm^2, ϵ_0 is the permittivity of vacuum, 8.85×10^{-12} F/m, and ϵ is the dielectric constant of aluminum oxide, 8.6[21]

$$C_{bl} = \epsilon\epsilon_0 A/d \qquad (1)$$

The capacitance of the barrier aluminum oxide layer was assumed to be equal to the magnitude of CPE_1 because the frequency dissipation factor (α_1) was almost equal to 1 (0.96 ± 0.01). Due to a slow rate of dissolution, the layer of barrier aluminum oxide was considered to be quasi-stable over the time period of EIS measurements (about 3 min). The EIS scan was repeated every 10 min. The left part of Figure 2 shows that the magnitude of CPE_1 increases and the thickness of the

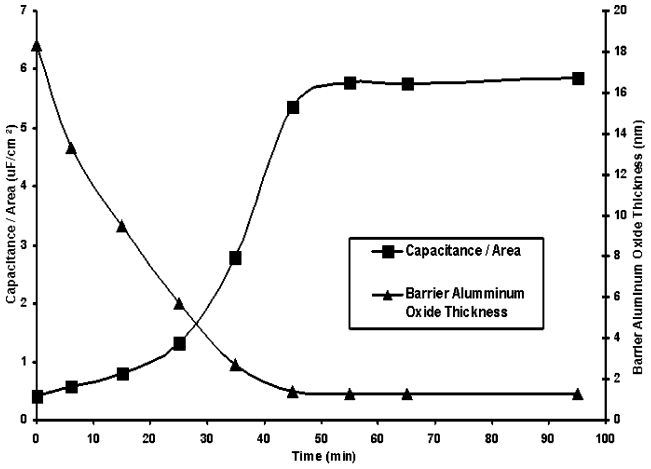

Figure 2. Capacitance and thickness of the layer of barrier aluminum oxide during etching.

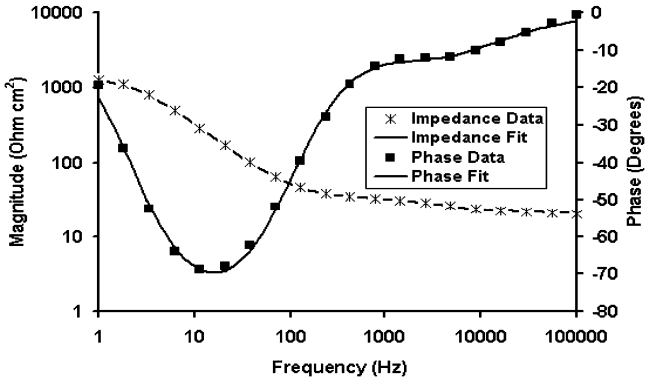

Figure 3. EIS data (magnitude of impedance and phase) collected at OCP after electroless deposition of silver for 3 h.

barrier aluminum oxide layer almost linearly decreases with time at a constant temperature. A constant dissolution rate of barrier aluminum oxide was a consequence of the constant electrode area exposed to the etching electrolyte. The etching was carried out for approximately 50 min after establishing that both the magnitude of CPE_1 and, as a result, thickness of barrier aluminum oxide did not vary with time. At this moment, the layer of barrier aluminum oxide was assumed to be thinnest, which favored the electroless deposition of silver.

Establishment of the utility of EIS allows us to employ this method to monitor the electroless deposition of silver. Figure 3 shows the Bode representation of an EIS spectrum collected after 180 min of electroless deposition of silver. Table 1 (right column) lists the results of modeling by using the same equivalent circuit as discussed above. Careful comparison of Figures 1 and 3 shows that the magnitude of total cell impedance significantly decreases and the phase becomes less negative in the low-frequency region between 1 and 500 Hz. As shown in Table 1 (right column), both of these observations result from an increased value of CPE_1 (by 1 order of magnitude) and a decreased value of R_1 (by 2 orders of magnitude). We conclude that the electroless silver deposition for 3 h transforms CPE_1 from being dominated by the thin (1.4 nm) layer of barrier aluminum oxide ($5-6\ \mu F/cm^2$)[21] to being dominated by the barrier aluminum oxide with silver particles on the top/electrolyte interface ($30-40\ \mu F/cm^2$).[27] Concurrently with increasing capacitance, the resistance of the layer of barrier aluminum oxide decreases from 100 $k\Omega\ cm^2$ to $1-2\ k\Omega\ cm^2$ (Table 1). This observation most likely results from the incorporation of silver in the layer of barrier aluminum oxide

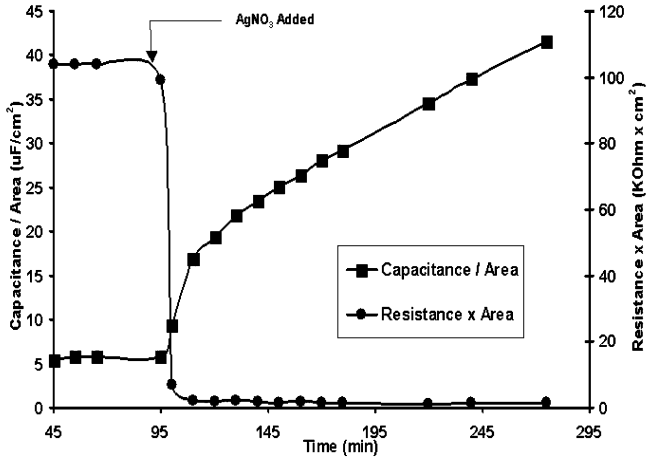

Figure 4. Capacitance and resistance of the layer of barrier aluminum oxide during electroless deposition of silver on aluminum/copper substrates. The time axis (Figure 4) is a continuation of the time axis (Figure 2) with some overlap between 45 and 100 min.

and, as a result, an increase in the electronic conductivity in this layer. Figure 4 demonstrates that after addition of $AgNO_3$ (the cell concentration of 1.1 mM) and a short incubation period, CPE_1 monotonically increases over the investigated period of time (3 h). In contrast, the resistance of barrier aluminum oxide (R_1) suddenly drops in the few first minutes of electroless deposition and slightly decreases afterward over 3 h. We note that neither element of the second (R_2 CPE_2) combination changes appreciably during electroless deposition. This observation confirms that this combination most likely originates from the barrier aluminum oxide/aluminum interface. As a result, the (R_2 CPE_2) combination is not influenced by electroless deposition, which takes place on the barrier aluminum oxide/electrolyte interface. Given the observed changes in both R_1 and CPE_1, we conclude that EIS is of great practical utility for in-situ monitoring of the silver electroless deposition.

To investigate the electroless deposition of silver, the galvanic displacement was interrupted after 9, 60, 120, and 180 min of continuous deposition. The silver deposits were examined by SEM (Figure 5a−d), respectively. The black pseudohexagonal spots with white edges shown in Figure 5a represent the scallops of barrier aluminum oxide left on the surface after anodization and etching. As observed from Figure 5a, the silver phase formation starts preferentially in the centers of scallops. We conclude that minimal thickness of barrier aluminum oxide facilitates the formation of silver particles. The thickness of the oxide layer is known to play a significant role in determining the location of nucleation sites during electroless and electrodeposition.[28] We note that no electroless deposition of silver was observed if the anodization and etching steps were omitted. The analysis of the micrographs revels that the electroless deposition proceeds via the formation of spherical particles of silver randomly distributed on the surface. Both the particle density and average particle diameter increase with the deposition time. The average diameter of particles increases from 50 nm after 9 min of deposition to 180 nm after 120 min. The fact that the electroless deposition results in a distribution of particle diameters indicates the silver phase formation is a continuous process (e.g., new nanoparticles are formed while old particles increase in diameter). By varying the duration and temperature of silver electroless deposition, it is possible to fabricate coatings containing silver particles with a variety of diameters. The chemical composition of the deposited particles was confirmed by EDS. Figure 6 shows an EDS spectrum collected after 180

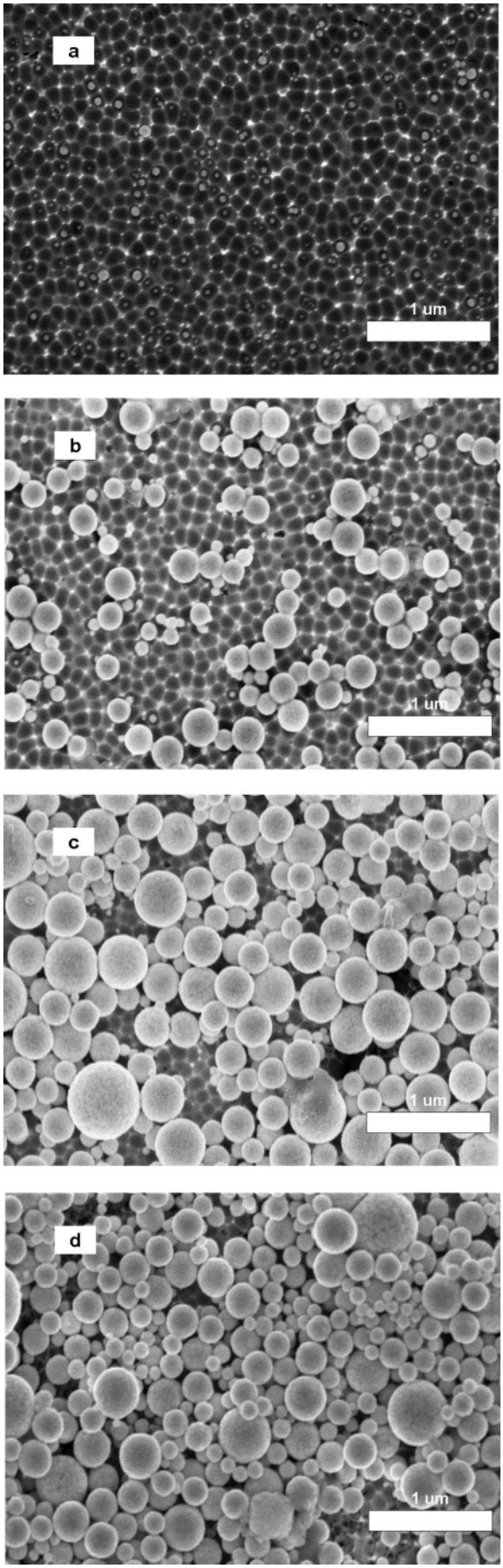

Figure 5. SEM micrographs collected after electroless deposition of silver for 9 min (a), 1 h (b), 2 h (c), and 3 h (d).

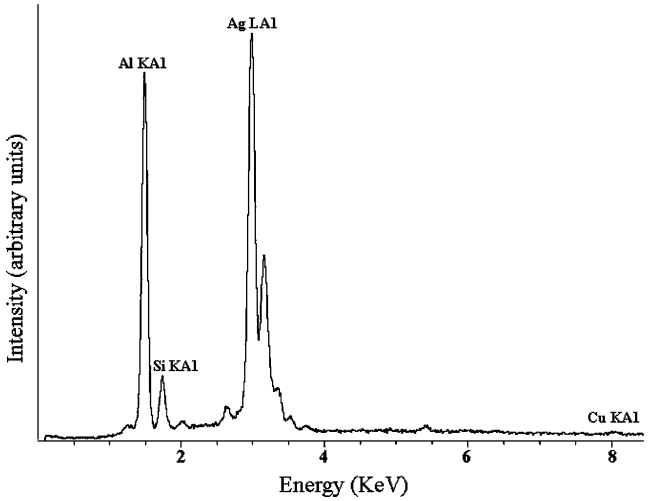

Figure 6. EDS spectrum collected after electroless deposition of silver for 3 h on 99.5% aluminum and 0.5% copper films.

min of electroless plating. The spectrum shows the presence of aluminum, silicon, silver, and a trace amount of copper.

To elucidate the mechanism of silver electroless deposition on 99.5% aluminum alloyed with 0.5% copper, control experiments were performed under the same conditions, but with pure (99.997%) aluminum foil (Alfa Aesar), as a substrate. These experiments demonstrated no increase in the interfacial capacitance over of a period of 2 h after addition of the same amount of $AgNO_3$. In addition, SEM examination of the samples revealed no particles of silver. Aluminum is known to be a stronger reducing agent than copper (the redox potential of Al^{3+}/Al is about 2.0 V more negative than that of Cu^{2+}/Cu). Therefore, the driving force for galvanic displacement of aluminum by silver is significantly larger than that of copper by silver (0.46 V). However, aluminum is also a very inert metal due to the presence of the surface oxide layer. Thus, it was not surprising that galvanic displacement of aluminum by silver was not observed under our experimental conditions (1.1 mM $AgNO_3$, a mixture of chromic and phosphoric acids, pH 1.8, 60 °C). These results confirm that the electroless deposition of silver on pure aluminum substrates is a kinetically prohibited process due the presence of the layer of barrier aluminum oxide, which prevents the charge transfer between the aluminum substrate and cations of silver.

EIS measurements at OCP indicate that magnitudes of CPE_1 and, as a result, the thickness of barrier aluminum oxide are approximately the same for both substrates (99.5% aluminum alloyed with 0.5% copper films and pure 99.997% aluminum). However, the substrates show a striking difference with respect to the electroless silver deposition. We suggest that by alloying aluminum with copper, carrying out anodization, and sequential chemical etching aluminum films are made amenable to electroless deposition of silver by galvanic displacement of copper. This phenomenon results from incorporation of metallic copper into and underneath the thin layer of barrier aluminum oxide, which makes the electron transfer to cations of silver possible. This statement is supported by the following observations. Upon completion of etching of aluminum/copper films in 0.4 M phosphoric and 0.2 M chromic acids (pH 1.8, 60 °C), OCP attained a sufficiently negative value of −0.70 V vs a Ag/AgCl reference electrode. On the other hand, oxidation of copper was reported to occur at approximately 0.0 V vs Ag/AgCl in a solution of sulfuric acid.[29] Upon the basis of these observations, one can conclude that the oxidation state of copper incorporated in the layer of barrier aluminum oxide is zero. In addition, in

aluminum/copper films, copper is cathodically protected by aluminum metal present in the bulk. Electroless deposition of silver by galvanic displacement on pure copper substrates was reported in the literature, despite the fact that authors did not directly mention the mechanism of deposition.[14] Our additional experiments also demonstrated that the elevated temperatures accelerated the electroless deposition of silver. At a room temperature, the electroless deposition was achievable but occurred at a slow rate as determined by EIS and SEM. For example, the electroless deposition of silver for 2 h at 22 °C increased the magnitude of CPE_1 to only 7−8 $\mu F/cm^2$. In contrast, the same increase was achieved after electroless deposition for only 4−5 min at 60 °C.

In contrast to results reported elsewhere,[30] we observed no electroless deposition of copper on aluminum/copper films after anodization and etching. The attempted deposition of copper was performed under the same conditions as deposition of silver. In these experiments, 3.0 mM Cu_2SO_4 in a mixture of phosphoric and chromic acids was used and the deposition time was over 30 min. Previously reported electroless deposition of copper was performed from organic solvents,[30] whereas our experiments were carried out in an aqueous solution. The combined observations in this report (silver deposition on anodized and etched aluminum/copper films, no silver deposition on anodized and etched aluminum, no copper deposition on anodized and etched aluminum/copper films) support our hypothesis that copper incorporated in the barrier aluminum oxide acts as a reducing agent for electroless deposition of silver. This hypothesis does not eliminate the possibility that aluminum and copper may form a galvanic couple. In this case, the oxidation of Cu by Ag(I) would be coupled to the oxidation of Al by Cu(II). This statement is indirectly supported by two observations. First, the analysis of the plating solution by inductively coupled plasma (ICP) atomic emission spectroscopy does not show any presence of copper upon completion of electroless deposition for 3 h. The detection limit of this method is 0.01 mg/L. Second, the electroless deposition results in a large amount of silver deposited on the aluminum/copper films. Given a small percentage of copper (0.5 wt %) in the film, it is reasonable to suggest that metallic copper is constantly replenished by reduction of CuO by aluminum. Considering these observations, it is possible to suggest that copper mediates the oxidation of aluminum by silver cations.

In summary, the electroless deposition of silver by galvanic displacement on 99.5% aluminum films containing 0.5% copper results in the formation of particle-type films of silver. Traditionally, zincating or stannating processes are used as the initial treatment of aluminum surfaces for sequential electroless or electrodeposition of metals (e.g., Ni).[10,11] The procedure reported here for electroless deposition of silver particles by galvanic displacement can be used as an alternative method to activate the aluminum films alloyed with copper. As a result of the activation, the aluminum surface can be further coated with a metal (e.g. Ni, Ag, and Au) by means of electroless or electrodeposition. In addition, methods have been reported for patterning and anodization of the aluminum films only in those areas, which do not have a protective mask.[31] A combination of these methods and electroless deposition of silver is attractive for selective metallization of aluminum surfaces. Future studies will focus on combining the electroless deposition and photolithographic methods in order to fabricate structures with particles of silver deposited only in selected areas.

Conclusions

We have described a novel procedure for electroless deposition of silver on films containing 99.5% aluminum and 0.5% copper. The deposition proceeds via the galvanic displacement mechanism by which silver cations are reduced and copper is oxidized. The electroless deposition by galvanic displacement does not take place with pure 99.997% aluminum substrates. Therefore, alloying aluminum with copper, anodization, and subsequent chemical etching (in order to minimize the thickness of surface aluminum oxide) make the electroless deposition of silver on aluminum/copper substrates possible. In addition, we have demonstrated that EIS is a convenient in situ method to follow the electroless deposition of silver. The electroless silver deposition for 3 h transforms the interfacial capacitance from being dominated by the thin layer of barrier aluminum oxide (5−6 $\mu F/cm^2$) to being dominated by the barrier aluminum oxide with incorporated silver/electrolyte interface (30−40 $\mu F/cm^2$). Scanning electron micrographs demonstrate that electroless deposition by the galvanic displacement mechanism results into the formation of particle-type films of silver. By varying the conditions for silver electroless deposition (e.g., duration and temperature), it is possible to fabricate silver particles with a range of diameters (10−200 nm).

Acknowledgment. This work was supported in part by the Army Research Office Grant DAAD 190210085 and the Center for Micro-Engineered Materials at the University of New Mexico. The SEM laboratory was supported by the New Mexico EPCoR NSF grant and the NNIN grant. We thank Todd M. Bauer (Sandia National Laboratories, Albuquerque, NM) for assistance with fabrication of silicon wafers with an aluminum−copper layer.

References and Notes

(1) Balashova, N. A.; Eletskii, V. V.; Medyntsev, V. V. *Elektrokhim.* **1965**, *1* (3), 235.

(2) Oskam, G.; Long, J. G.; Natarajan, A.; Searson, P. C. *J. Phys. D−Appl. Phys.* **1998**, *31* (16), 1927.

(3) Magagnin, L.; Maboudian, R.; Carraro, C. *J. Phys. Chem., B* **2002**, *106* (2), 401.

(4) Porter L. A.; Choi H. C.; Ribbe A. E.; Buriak J. M. *Nano Lett.* **2002**, *2* (10), 1067.

(5) Dubin, V. M.; Shacham-Diamand, Y.; Zhao, B.; Vasudev, P. K.; Ting, C. H.; *J. Electrochem. Soc.* **1997**, *144* (3), 898.

(6) Hsu, H. H.; Hsieh, C. C.; Chen, M. H.; Lin, S. J.; Yeh, J. W. *J. Electrochem. Soc.* **2001**, *148* (9), C590.

(7) Wang, Z.; Ida, T.; Sakaue, H.; Shingubara, S., T. Takahagi, T. *Electrochem. Solid-State Lett.* **2003**, *6* (3), C38.

(8) Carraro, C.; Magagnin, L.; Maboudian, R. *Electrochim. Acta* **2002**, *47* (16), 2583.

(9) Djokic, S. S. *J. Electrochem. Soc.* **1996**, *143* (4), 1300.

(10) Stoyanova, E.; Stoychev, D. *J. Appl. Electrochem.* **1997**, *27* (6), 685.

(11) Hutt, D. A.; Liu, C.; Conway, P. P.; Whalley, D. C.; Mannan, S. H. *IEEE Trans. Compon. Packag. Technol.* **2002**, *25* (1), 87.

(12) Watanabe, H.; Honma, H. *J. Electrochem. Soc.* **1997**, *144* (2), 471.

(13) Karpinski, A. P.; Russell, S. J.; Murphy, J. P. *J. Power Sources* **2000**, *91*, 77.

(14) Nie, C. S.; Feng, Z. *Appl. Spectrosc.* **2002**, *56* (3), 300.

(15) Chumanov, G.; Sokolov, K.; Gregory, B. W.; Cotton, T. M. *J. Phys. Chem.* **1995**, *99* (23), 9466.

(16) Yang, J.; Chen, S. H. *Appl. Spectrosc.* **2001**, *55* (4), 399.

(17) Parfenov, A.; Gryczynski, I.; Malicka, J.; Geddes, C. D.; Lakowicz, J. R. *J. Phys. Chem. B* **2003**, *107* (34), 8829.

(18) Jana, N. R.; Sau, T. K.; Pal, T. *J. Phys. Chem. B* **1999**, *103* (1), 115.

(19) Djokic, S. S. *J. Electrochem. Soc.* **2004**, *151* (6), C590.

(20) Jensen, T. R.; Malinsky, M. D.; Haynes, C.; Van Duyne, R. P. *J. Phys. Chem. B* **2000**, *104* (45), 10549.

(21) Brevnov, D. A.; Rama Rao, G. V.; López, G. P.; Atanassov, P. B. *Electrochim. Acta* **2004**, *49*, 2487.

(22) Hoar, T. P.; Wood, G. C. *Electrochim. Acta* **1962**, *7*, 333.

(23) Burleigh, T. D.; Smith, A. T. *J. Electrochem. Soc.* **1991**, *138* (8), L34.

(24) De Laet, J.; Terryn, H.; Vereecken, J. *Electrochim. Acta* **1996**, *41*, 1155.

(25) Oh, H. J.; Kim, J. G.; Jeong, Y. S.; Chi, C. S. *Jpn. J. Appl. Phys.* **2000**, *39* (12A), 6690.

(26) Tuccio, G.; Piazza, S.; Sunseri, C.; Di Quarto, F. *J. Electrochem. Soc.* **1999**, *146* (2), 493.

(27) Bard, A. J.; Faulkner, L. R. *Electrochemical Methods: Fundamentals and Applications*; John Willey: New York, 1980; pp 500−502.

(28) Radisic, A.; Oskam, G.; Searson, P. C. *J. Electrochem. Soc.* **2004**, *151* (6), C369.

(29) Moreira, A. H.; Benedetti, A. V.; Cabot, P. L.; Sumodjo, P. T. A. *Electrochim. Acta* **1993**, *38*, 981.

(30) Fang, R.; Gu, H.; O'Keefe, M. J.; O'Keefe, T. J.; Shin, W.-S.; Leedy, K. D.; Cortez, R. *J. Elec. Mater.* **2001**, *30* (4), 349.

(31) Brevnov, D. A.; Barela, M.; Piyasena, M. E.; López, G. P.; Atanassov, P. B. *Chem. Mater.* **2004**, *16*, 682.